Pathology of the emerging *Mycobacterium tuberculosis* complex pathogen, *M. mungi,* in the banded mongoose (*Mungos mungo*)

Kathleen A. Alexander [1, 2*], Peter N. Laver[1], Mark C. Williams[3], Claire E. Sanderson[1, 2], Carly Kanipe[4, 5], and Mitchell V. Palmer[5]

[1] Department of Fish and Wildlife Conservation, Virginia Tech, Blacksburg, Virginia

[2] CARACAL, Centre for Conservation of African Resources: Animals, Communities, and Land Use, Kasane, Botswana

[3] Section of Pathology, Department of Paraclinical Sciences, Faculty of Veterinary Science, University of Pretoria, Onderstepoort, South Africa

[4] Department of Veterinary Pathology, College of Veterinary Medicine, Iowa State University, Ames, Iowa

[5] Bacterial Diseases of Livestock Research Unit, National Animal Disease Center, Ames, Iowa

Corresponding author: Kathleen A. Alexander, Virginia Tech, Integrated Life Sciences Building 1981 Kraft Drive, Blacksburg, VA, USA 24060, phone: 540/231-5059, fax: 540/231-7580, email: kathyalx@vt.edu

Keywords: banded mongoose, emerging infectious diseases, environmental pathogen, *Mycobacterium mungi*, olfactory communication, transmission, tuberculosis, wildlife pathology

Abstract

Wild banded mongooses (*Mungos mungo*) in northeastern Botswana and northwest Zimbabwe are infected with a novel *Mycobacterium tuberculosis* complex (MTC) pathogen, *M. mungi.* We evaluated gross and histologic lesions in 62 infected mongooses (1999-2017). Many tissues contained multifocal irregular, lymphohistiocytic to granulomatous infiltrates and/or multifocal or coalescing non-caseating to caseating granulomas with variable numbers of intralesional acid fast bacilli. Over 1/3 of nasal turbinates examined had submucosal lymphohistiocytic to granulomatous infiltrates, erosion and ulceration of the nasal mucosa, bony remodeling, and nasal distortion. Similar inflammatory cell infiltrates expanded the dermis of the nasal planum with frequent ulceration. However, even in cases with intact epidermis, acid-fast bacilli were present in variable numbers among dermal infiltrates and on the epidermal surface among desquamated cells and debris, most commonly in small crevices or folds. In general, tissue involvement varied among cases but was highest in lymph nodes (50/54, 93%), liver (39/53, 74%), spleen (37/51, 73%), and anal glands/sacs (6/8, 75%). Pulmonary lesions were present in 67% of sampled mongooses (35/52) but only in advanced disseminated disease. The pathological presentation of *M. mungi* in the banded mongoose is consistent with pathogen shedding occurring through scent-marking behaviours (urine and anal gland secretions) with new infections arising from contact with these contaminated olfactory secretions and percutaneous movement of the pathogen through breaks in the skin, nasal planum, and/or skin of the snout. Given the character and distribution of lesions and the presence of intracellular acid fast bacilli,

we hypothesize that pathogen spread occurs within the body through a hematogenous and/or lymphatic route. Features of prototypical granulomas such as multinucleated giant cells and peripheral fibrosis were rarely present in affected mongooses. Acid fast bacilli were consistently found intracellularly, even in regions of necrosis. The mongoose genome has a unique deletion (RD1^{mon}) that includes part of the encoding region for PPE68 (Rv3873), a gene co-operonic with PE35. These proteins can influence the host's cellular immune response to mycobacterial infections and it remains uncertain how this deletion might contribute to observed patterns of pathology. *M. mungi* infection in banded mongooses is characterized by both a unique transmission and exposure route, and accompanying pathological features, providing an opportunity to increase our understanding of MTC pathogenesis across host-pathogen systems.

Introduction

Mycobacterium mungi is a newly-discovered emerging tuberculosis (TB) pathogen within lineage six of the *M. tuberculosis complex* (MTC)[2]. *M. mungi* is closely related to *M. africanum* West African 2 *(Maf 2),* a significant cause of TB among humans in West Africa.[3,20] *M. mungi* infects banded mongoose (*Mungos mungo*) populations in northeastern Botswana and northwest Zimbabwe.[4] Banded mongooses are small, cooperative breeding carnivores with a wide distribution in Africa.[4]

M. mungi was confirmed as a member of the MTC through full genome sequencing, placing the organism in the lineage six wildlife-associated group,[2,3] together with *M. suricattae* (meerkats, *Suricata suricatta*[22]), Dassie bacillus (rock hyrax, *Procavia capensis*[24]), and chimpanzee bacillus (chimpanzee, *Pan troglodytes* ssp[8]). Previously, MIRU-VNTR analyses of *M. mungi* isolates identified substrains within and between mongoose troops and sample years, indicating possible evolution of the organism over time and transmission complexity among mongoose social groups.[2] Evidence presently suggests that the banded mongoose is the definitive host; the full host spectrum, however, remains unknown.

M. mungi has many unique ecological characteristics that set it apart from other members of the MTC complex. First, *M. mungi* causes significant mortality among banded mongooses with disease-mediated losses threatening the persistence of smaller social groups experiencing other sources of mortality and group size depression. Second, rather than relying on primary aerosol or oral transmission routes,

as is characteristic of most other MTC species, *M. mungi* is transmitted via an environmental pathway through infected urine and anal gland secretions.[4] These secretions are used in olfactory communication behavior with pathogen invasion occurring through breaks in the skin, nasal planum, and/or snout of the mongoose host. Such a mode of transmission would allow the pathogen to spread between social groups where territorial behavior would normally limit contact and would potentially allow transmission among troops across a landscape. Third, the disease outbreaks have a seasonal pattern with onset in the dry season (April-October) and, generally, few cases in the wet season (November-May) [5], although an increasing number of cases are now occurring in the wet season. Lastly, the period between clinical presentation and death in affected mongooses is generally short (< 3 months) as compared with other MTC pathogens where infection can last years.[21]

Since the first outbreak in 1999, 93% (14/15) of radio-tracked and intensively studied troops are now infected. The prevalence of *M. mungi* disease within mongoose troops currently ranges from 3% to 17% (7.3 ± 4.4%, mean ± SD) of the total troop, including pups and juveniles, although, historically, disease incidence has been as high as 37.5%. The 15th intensively studied group has not shown any evidence of infection over the last 18 years of observations and is not obviously isolated by any geographical barriers from surrounding troops.

The objective of the present study was to evaluate the pathological presentation of *M. mungi* infection in the banded mongoose host in relation to the unique mechanisms of

pathogen shedding and transmission observed in this emerging MTC species. We compared pathological presentation to other lineage-six, wildlife-associated organisms, *M. bovis*, and *M. tuberculosis* and their hosts and discuss implications to our understanding of the pathogenesis of *M. mungi* infection.

Materials and Methods

In Chobe District, Botswana (approximately 25.163°E and 17.828°S), banded mongoose troops have been the focus of a long-term study since 2000 after the discovery of *M. mungi* in 1999.[2] In each troop, one to two animals were radio-collared and troops were monitored weekly for infection and other variables as previously described.[2] Necropsies were performed on opportunistically obtained banded mongoose carcasses found in the study area during this same period (hit by car, attacked by dogs, killed by wildlife management officers, etc.). Samples of all major organs and any macroscopically visible lesions were collected and fixed in 10% buffered formalin for histological examination. Tissue availability varied among necropsies according to the condition of the carcass being examined. Formalin-fixed tissue sections were prepared using routine techniques and stained with hematoxylin and eosin (HE). A Ziehl-Neelsen (ZN) staining method was used to visualize acid-fast bacilli (AFB). Infection status was additionally confirmed by PCR as previously described.[4]

Ethical Treatment of Animals

All animal handling and sampling activities in this study were conducted under approval from the Virginia Tech Institutional Animal Care and Use committee [IACUC 13-164-FIW], as well as the Botswana Ministry of Environment, Wildlife, and Tourism [EWT 8/36/4 XXVI (24)].

Results

We evaluated gross pathologic and histopathologic findings associated with *M. mungi* infection in 62 banded mongooses (1999-2017). Positive infection status was determined through gross examination (lesions consistent with mycobacteriosis), histology (presence of AFB), and PCR (detection of *M. mungi*-specific DNA). At present, there are no ante-mortem diagnostics available for diagnosis of *M. mungi* infection. There was no statistical difference in infection levels between males and females (χ^2(1, N = 184); p=.32). It was not possible to estimate the percentage of affected mongooses sampled in this study as the population size and total number affected fluctuated over time and could not be accurately estimated. Clinical signs in *M. mungi*-infected mongooses included fearlessness, lethargy, lagging behind the group, severe weight loss, hunched body posture, matted fur, drooping and/or enlarged testicles, epiphora, nasal distortion, rhinorrhea, and sneezing.

Gross Lesions

Nasal distortion was commonly identified with occasional erosion of the nasal planum (Fig. 1). Erosion of the hard palate was noted in two cases (Fig. 2). In most animals, lymph nodes were enlarged, pale, with multifocal necrosis and indistinct separation of

Figures 1–3. Mycobacterium mungi infection, banded mongoose.

Figure 1. Ulceration of the nasal planum.
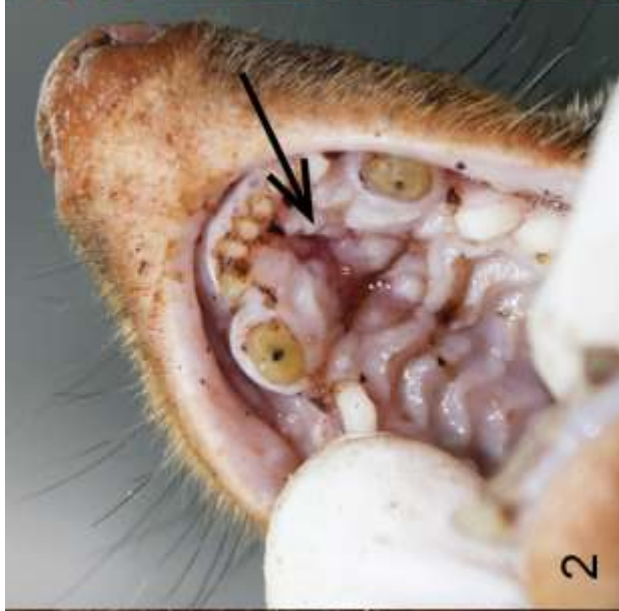
Figure 2. Erosion of the hard palate.
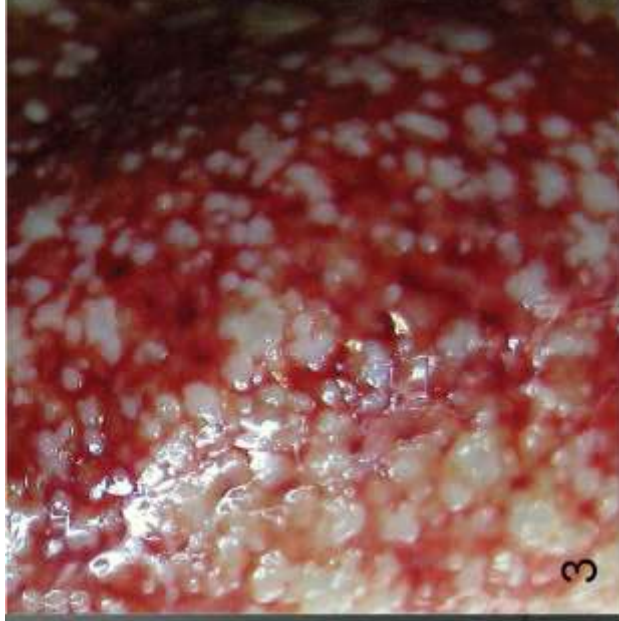
Figure 3. Liver. Extensive miliary gray-white nodular 0.1- to 2-cm diameter masses were present on the capsular surface and within the parenchyma.
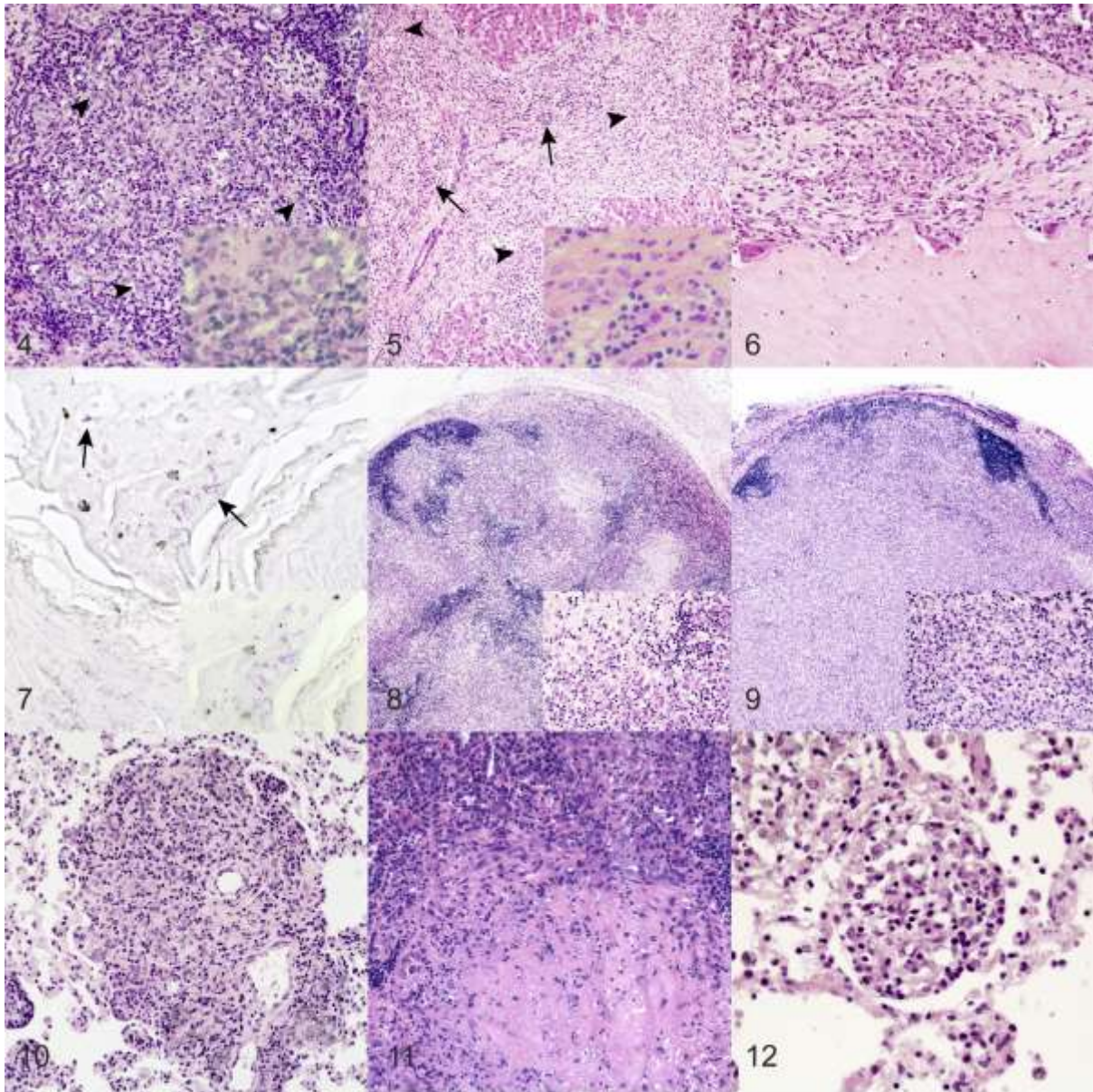
cortex and medulla. Lungs, liver, spleen, and kidney had focal to multifocal pale nodular to irregular masses (0.1 cm–2 cm in diameter) on the capsular or pleural surface as well as on the cut surface (Fig. 3).

Microscopic lesions

Among the 62 infected mongooses, 806 separate tissues were examined microscopically. Tissue involvement varied among affected mongooses but was highest in lymph nodes (50/54 mongooses, 93%), liver (39/53, 74%), spleen (37/51, 73%), and anal glands/sacs (6/8, 75%; Table 1). Tissue changes were characterized by the presence of irregular lymphohistiocytic (unorganized infiltrates of roughly equal numbers of lymphocytes and macrophages) to granulomatous infiltrates (macrophages and activated epithelioid macrophages with fewer lymphocytes, arranged in variably sized aggregates or sheets) or multifocal to coalescent non-caseating to caseating granulomas. In general, organs (liver, spleen, kidney, adrenal gland, salivary glands, pancreas, stomach, intestines, and bladder) had multifocal, nodular to irregular non-caseating granulomas with infiltrates of macrophages, epithelioid macrophages, lesser numbers of lymphocytes, and rare multinucleated giant cells arranged in round to oval fashion (Fig. 4). Outermost regions of the nodular arranged infiltrates were more lymphocyte-rich than central regions. In other cases, mild to moderate central necrosis was identified (caseating granuloma). Mineralization and peripheral fibrosis were absent. Three affected livers had multifocal, bridging-portal, lymphohistiocytic inflammation with mild to moderate fibrosis (Fig. 5). In all tissues, AFB were variable in number.

Table 1. Lesion distribution in 62 Mycobacterium mungi infected banded mongoose (*Mungos mungo*). Lesions consistent with mycobacteriosis are reported by tissue. Only tissues for which at least five animals were examined are included. Listed in descending order of number of tissues with lesions.

Tissue	Number examined	Number with lesions	% Lesions
Lung	52	35	67
Liver	53	39	74
Lymph nodes	54	50	93
Spleen	51	37	73
Kidney	47	15	32
Nasal mucosa and turbinates	27	10	37
Nasal planum (skin)	39	15	38
Haired skin (location unknown)	13	6	46
Perianal gland	8	6	75
Perianal skin	7	4	57
Testicle	18	4	22
Adrenal gland	26	9	35
Epididymis	13	4	31
Stomach	9	2	22
Small intestine	13	2	15
Salivary gland	28	2	7
Large intestine	11	1	9
Bladder	15	1	7
Pancreas	14	1	7.1
Heart	27	1	4
Uterus	5	0	0

Figures 4–12. Mycobacterium mungi infection, banded mongoose.

Figure 4. Kidney. Granuloma composed of macrophages and lymphocytes, with the outer zone being more lymphocyte-rich. Histiocytes are indicated with arrowheads. Inset: higher magnification of lymphocytes and macrophages within the granulomas. Hematoxylin and eosin (HE).

Figure 5. Liver. Lymphohistiocytic infiltrates and fibrosis bridge the portal regions. Histiocytes are indicated with arrowheads and lymphocytes are indicated with arrows. Inset: higher magnification of portal inflammation. HE.

Figure 6. Nasal turbinate. Bone has scalloped edges with several multinucleated osteoclasts and periosteal fibrosis. HE.

Figure 7. Epidermis, snout. Numerous acid-fast bacilli (indicated with arrows) are present within desquamated epithelial cells. Inset: higher magnification of acid-fact organisms. Ziehl-Neelsen stain (ZN).

Figure 8. Medial retropharyngeal lymph node. Multifocal to coalescent granulomas composed of macrophages and lymphocytes contain central areas of necrosis. Inset: higher magnification of inflammatory cells. HE. F

Figure 9. Popliteal lymph node. The architecture is effaced by sheets of macrophages and lesser numbers of lymphocytes. Inset: higher magnification of inflammation. HE.

Figure 10. Lung. Granulomatous infiltrates surround several pulmonary vessels. HE.

Figure 11. Lung. Caseonecrotic granuloma. HE.

Figure 12. Lung. Nodular aggregate of macrophages and lymphocytes within an alveolar space. HE.

Of 27 nasal turbinates examined, 10 (37%) had submucosal lymphohistiocytic to granulomatous infiltrates. Erosion and ulceration of the nasal mucosa was commonly noted. Multifocally, nasal turbinate bone had scalloped edges and periosteal fibrosis characteristic of bony remodeling (Fig. 6). Intracellular AFB were frequently located in macrophages in submucosal inflammatory lesions. Similar infiltrates expanded the dermis of the nasal planum. The epidermis of the nasal planum was ulcerated in 38% (15/39) of the cases in which it was examined, with moderate numbers of neutrophils and fibrin associated with the ulcerated areas. Even in cases with intact epidermis, AFB were present in variable numbers among dermal infiltrates and in small numbers among desquamated cells and debris on the epidermal surface, most commonly in small crevices or folds (Fig. 7). Similar dermal and epidermal lesions with surface AFB were detected in sampled skin lesions (6/13, 46%) and scrotum (2/4, 50%). In some cases, testicular and epididymal involvement included multifocal to diffuse granulomatous infiltrates that effaced normal tissue architecture in more advanced lesions. The number of AFB in testicular and epididymal lesions ranged from few to myriad.

A total of 605 lymph nodes from 63 infected mongooses were examined including the mandibular, mesenteric, superficial cervical, inguinal, popliteal, anal, medial retropharyngeal, lumbar, mediastinal, gastric, hepatic, and parotid lymph nodes. Lymph node lesions were characterized by multifocal to coalescent non-caseating to caseating granulomas (Fig. 8) or focally extensive granulomatous infiltrates arranged in sheets of cells (mostly macrophages) that effaced normal lymph node architecture (Fig. 9). While

necrosis was observed in approximately one third of granulomas, peripheral fibrosis was not a feature of lymph node lesions and dystrophic mineralization of necrotic caseum was only rarely seen (two cases). Irrespective of the anatomic location of the lymph nodes examined, or the stage of disease, the lesion size and severity were generally consistent among all lymph nodes in an infected mongoose.

Pulmonary lesions were found in 67% (35/52) of lungs examined and were characterized as disseminated, nodular (30-500 µm) lymphohistiocytic to granulomatous infiltrates, or non-caseating to caseating granulomas. Pulmonary lesions were mainly present in animals with disseminated disease. In 94% (33/35) of the cases where pulmonary lesions were identified, at least one other primary organ (i.e., liver, spleen, or kidney) contained lesions suggestive of hematogenous or lymphatic dissemination of the pathogen. Of the 2 cases without involvement of liver, spleen, or kidney, 1 had similar lesions in multiple lymph nodes and the anal glands/sacs consistent with hematogenous or lymphatic dissemination.

Microscopic lesions within the affected lung were of three general types. The first was characterized by perivascular and subpleural distribution of lymphohistiocytic to granulomatous infiltrates that varied from individually separated nodules to expansile coalescing lesions (Fig. 10). Perivascular and peribronchiolar macrophages often contained darkly colored, granular material suggestive of silicosis. The second lesion type presented as multifocal, non-caseating to caseating granulomas with no apparent vasocentric or bronchocentric distribution (Fig. 11). The third lesion type was

characterized by small nodular lymphohistiocytic infiltrates within the alveolar interstitiumsepta, which filled variable amounts of the alveolar space (Fig. 12). Intracellular AFB were noted in all lesion types. It was noteworthy that even in necrotic foci, AFB were invariably intracellular and not free within the necrotic caseum. Other infrequent findings in the lungs were focal to multifocal hemorrhages, pulmonary edema, and nematode parasites within bronchiolar lumens.

Anal gland and sac tissue often contained lymphohistiocytic to granulomatous infiltrates with large numbers of AFB (6/8, 75%). The keratinized surface of the duct of the anal sac contained small numbers of AFB in cellular debris found in small superficial epidermal crevices, as well as within the epidermis itself.

Discussion

M. mungi-infected banded mongoose had the highest number of lesions in the lymph nodes, liver, spleen, and anal glands/sacs with the lung only involved in cases of advanced disease. In other MTC hosts, including humans and animals, aerosol transmission is believed to be the primary route of pathogen transmission. In these species, lesions centered on airways (i.e., bronchi and bronchioles) predominate, and lesion expansion, airway invasion, and expulsion of bacilli through breathing or coughing is critical to disease transmission. In mongooses infected with *M. mungi*, a different picture emerges. While tuberculous lesions were common in the lungs of severely affected mongooses, these were centered around pulmonary vasculature rather than associated with the bronchi or bronchioles, suggesting hematogenous or

lymphatic dissemination to and within the lung. Common involvement of the lymph nodes, liver, and spleen are also consistent with hematogenous or lymphatic spread acting as the primary mechanism of pathogen movement within the mongoose host. Consistent with pathogen shedding occurring through infected anal gland and urine secretions[4], granulomatous lesions with AFB were seen in 75% of the anal gland/sac tissues and 32% of the kidneys of infected animals.

Lymphohistiocytic to granulomatous lesions were seen in 37% of the nasal cavities examined in *M. mungi* infected banded mongoose. Upper respiratory lesions are uncommon in tuberculosis caused by other MTC pathogens, such as *M. tuberculosis* and *M. bovis*.[14] In humans, primary nasal tuberculosis is exceedingly rare with only 40 cases reported worldwide.[14] Granulomatous lesions were also found in the skin of the nasal planum. Lesions in the nasal cavity and on the nasal planum could result from mongooses sniffing scent marks containing *M. mungi* organisms (urine and/or anal gland secretions) or foraging in the soil in locations where *M. mungi* containing secretions have been deposited. The presence of AFB in the crevices and hair follicles of intact skin, nose, scrotum, anal sac, anal canal, and perineum are consistent with anal marking behavior of mongooses where anal gland secretions are placed directly on conspecifics or used in over-marking behaviors, where mongooses will deposit anal gland secretions on other anal marks of potentially infected mongooses.

The hallmark lesion of tuberculosis in natural hosts is the granuloma. The prototypical tuberculoid granuloma has a central region of caseous necrosis, which may contain foci

of mineralization, surrounded by a zone of epithelioid macrophages and multinucleated giant cells, with the outermost zone containing increasing numbers of lymphocytes. The entire mass of necrotic caseum and inflammatory cells is often encased in a fibrous capsule of variable thickness.[1] *M. mungi*-induced lesions differed slightly in that multinucleated giant cells were rarely present and peripheral fibrosis was lacking. Such findings have also been features of *M. bovis*-induced lesions in Eurasian badgers (*Meles meles*), brushtail possums (*Trichosurus vulpecula*), and meerkats.[11,13,19]

In MTC-susceptible species where aerosol is the primary route of infection, secondary routes can include oral and percutaneous transmission (e.g., bite wounds). Cutaneous and subcutaneous granulomas are commonly observed in the Eurasian badger and are thought to be the result of fighting and biting behaviors.[7] Cutaneous lesions may also be associated with draining sinuses from affected superficial lymph nodes. Such lesions have been reported in *M. suricattae*-infected meerkats, and *M. bovis*-infected brushtail possums, fallow deer (*Dama dama*), and red deer (*Cervus elaphus*).[6,15] Although cutaneous and subcutaneous granulomatous inflammation was seen in mongooses examined in this study, draining sinuses from affected superficial lymph nodes were not observed.

M. mungi infection in the mongoose host was characterized by lymphohistiocytic to granulomatous inflammation, as well as the presence of caseating and non-caseating granulomas. Features common in prototypical granulomas, such as multinucleated giant cells and peripheral fibrosis, were rarely present. Moreover, AFB were consistently

found intracellularly, even in regions of necrosis. This contrasts with many other species where necrotic caseum often contains large numbers of both free and intracellular bacilli. Fibrous encapsulation of granulomas is generally considered to be a sign of disease control or healing, while expansion of necrosis with little or no encapsulation is considered a sign of disease progression.[12,17] In the zebrafish (*Danio rerio*) model of human tuberculosis, *M. tuberculosis*-infected macrophages migrate within a granuloma, as well as exit the granuloma to produce secondary granulomas and disseminated disease.[9] In similar fashion, macrophages with intracellular bacilli may escape poorly encapsulated granulomas in *M. mungi*-infected mongoose, resulting in disease dissemination and progression.

Differences in lesion morphology and disease progression may be related to genetic variations, such as the unique deletion in the *M. mungi* genome, RD1[mon].[5] The RD1[mon] deletion is comparatively small (1610 bp) when compared to other RD1 deletions in MTC organisms (RD1[das]/RD1[sur], 4132 bp; RD1[BCG], 9456 bp; RD1[mic],14120 bp).[4,10,16,18,23] The RD1[mon] deletion encompasses part of the encoding region for PPE68 (Rv3873), a gene present in both lineage six dassie bacillus and *M. suricattae.* PPE68 is co-operonic with gene PE35, and together these gene products have an important immunomodulatory role on host-pathogen interactions, influencing cellular immune responses to mycobacterial infections.[25] Experimentally, PPE68/PE35 is seen to increase levels of anti-inflammatory cytokine interleukin (IL)-10 and chemokine monocyte chemoattractant protein-1 (MCP-1).[4,25] Evidence suggests that this interaction may control granuloma formation regulating the pathophysiology in *M. tuberculosis*

infections[25], possibly contributing to the more unique pathological features of *M. mungi* infection in the banded mongoose.

M. mungi infection in banded mongoose is characterized by both a unique transmission and exposure route, and accompanying pathological features, providing an opportunity to increase our understanding of MTC pathogenesis across host-pathogen systems. An important area of future research is the examination of the potential role of the unique RD1^{mon} deletion in the pathophysiology of *M. mungi* infection in the banded mongoose host.

field and lab investigations, and A. Lasley, J. Wiarda, J. Stasko, and V. Montgomery

from the Bacterial Diseases of Livestock Research Unit, National Animal Disease

Center, for their technical assistance. The authors have no competing interests.

Figure Legends

Figures 1 – 3. *Mycobacterium mungi* infection, banded mongoose. Figure 1. Ulceration

of the nasal planum. Figure 2. Erosion of the hard palate. Figure 3. Liver. Extensive

miliary gray-white nodular 0.1–2 cm diameter masses were present on the capsular

surface and within the parenchyma.

Figures 4 – 12. *Mycobacterium mungi* infection, banded mongoose. Figure 4. Kidney.

Granuloma composed of macrophages and lymphocytes, with the outer zone being

more lymphocyte-rich. Histiocytes are indicated with arrowheads. Inset- higher

magnification of lymphocytes and macrophages within the granulomas. Hematoxylin

and eosin (HE). Figure 5. Liver. Lymphohistiocytic infiltrates and fibrosis bridge the

portal regions. Histiocytes are indicated with arrowheads and lymphocytes are indicated

with arrows. Inset - higher magnification of portal inflammation. HE. Figure 6. Nasal

turbinate. Bone has scalloped edges with several multinucleated osteoclasts and

periosteal fibrosis. HE. Figure 7. Epidermis, snout. Numerous acid-fast bacilli (indicated

with arrows) are present within desquamated epithelial cells. Inset - higher magnification

of acid-fact organisms. Ziehl-Neelsen stain (ZN). Figure 8. Medial retropharyngeal

lymph node. Multifocal to coalescent granulomas composed of macrophages and

lymphocytes contain central areas of necrosis. Inset- higher magnification of inflammatory cells. HE. Figure 9. Popliteal lymph node. The architecture is effaced by sheets of macrophages and lesser numbers of lymphocytes. Inset- higher magnification of inflammation. HE. Figure 10. Lung. Granulomatous infiltrates surround several pulmonary vessels. HE. Figure 11. Lung. Caseonecrotic granuloma. HE. Figure 12. Lung. Nodular aggregate of macrophages and lymphocytes within an alveolar space. HE.

References

1 Ackermann M: Inflammation and healing. *Pathologic basis of veterinary disease.* St Louis: Elsevier Mosby; 2012:89.

2 Alexander KA, Laver P, Michel A, Williams M, Van Helden P, Warren R, et al.: Novel *Mycobacterium tuberculosi*s complex pathogen, *M. mungi*. Emerging Infectious Diseases 2010:16(8):1296-1299.

3 Alexander KA, Larsen MH, Robbe-Austerman S, Stuber TP, Camp PM: Draft genome sequence of the *Mycobacterium tuberculosis* complex pathogen M. mungi, identified in a banded mongoose (*Mungos mungo*) in northern Botswana. *Genome Announcements* 2016:4(4):e00471-00416.

4 Alexander KA, Sanderson CE, Larsen MH, Robbe-Austerman S, Williams MC, Palmer MV: Emerging Tuberculosis Pathogen Hijacks Social Communication Behavior in the Group-Living Banded Mongoose (*Mungos mungo*). *mBio* 2016:7(3):e00281-00216.

5 Alexander KA, Sanderson CE, Laver PN: *Mycobacterium tuberculosis* complex spp. in group-living African mammals. In: Mukundan H, Chambers MA, Waters WR, Larsen MH, eds. *Many Hosts of Mycobacteria Tuberculosis, Leprosy, and other Mycobacterial Diseases of Man and Animals.* New York: CABI Publishers; 2014.

6 Amato B, Mignacca SA, Pacciarini ML, Vitale M, Antoci S, Cucinotta S, et al.: An outbreak of bovine tuberculosis in a fallow deer herd (*Dama dama*) in Sicily. *Res Vet Sci* 2016:106:116-120.

7 Corner L, Murphy D, Gormley E: *Mycobacterium bovis* infection in the Eurasian badger (*Meles meles*): the disease, pathogenesis, epidemiology and control. *Journal of Comparative Pathology* 2011:144(1):1-24.

8 Coscolla M, Lewin A, Metzger S, Maetz-Rennsing K, Calvignac-Spencer Sb, Nitsche A, et al.: Novel *Mycobacterium tuberculosis* complex isolate from a wild chimpanzee. *Emerging Infectious Diseases* 2013:19(6):969.

9 Davis JM, Ramakrishnan L: The role of the granuloma in expansion and dissemination of early tuberculous infection. *Cell* 2009:136(1):37-49.

10 Dippenaar A, Charles Parsons SD, Sampson SL, Gerhard van der Merwe R, Drewe JA, Abdallah AM, et al.: Whole genome sequence analysis of *Mycobacterium suricattae*. *Tuberculosis* 2015:95:682-688.

11 Drewe J, Foote A, Sutcliffe R, Pearce G: Pathology of *Mycobacterium bovis* infection in wild meerkats (*Suricata suricatta*). *Journal of Comparative Pathology* 2009:140(1):12-24.

12 Hunter RL: Pathology of post primary tuberculosis of the lung: an illustrated critical review. *Tuberculosis* 2011:91(6):497-509.

13 Jackson R, Cooke M, Coleman J, Morris R, Yates G: Naturally occurring tuberculosis caused by *Mycobacterium bovis* in brushtail possums (*Trichosurus vulpecula*): III. Routes of infection and excretion. *New Zealand Veterinary Journal* 1995:43(7):322-327.

14 Khan S, Pujani M, Jetley S: Primary nasal tuberculosis: Resurgence or coincidence− A report of four cases with review of literature. *Journal of Laboratory Physicians* 2017:9(1):26.

15 Lugton IW, Wilson PR, Morris RS, Nugent G: Epidemiology and pathogenesis of *Mycobacterium bovis* infection of red deer (*Cervus elaphus*) in New Zealand. *New Zealand Veterinary* Journal 1998:46(4):147-156.

16 Mahairas GG, Sabo PJ, Hickey MJ, Singh DC, Stover CK: Molecular analysis of genetic differences between *Mycobacterium bovis* BCG and virulent *M. bovis*. *Journal of Bacteriology* 1996:178(5):1274-1282.

17 Martin CJ, Carey AF, Fortune SM: A bug's life in the granuloma. *Seminars in immunopathology*: Springer; 2016: 213-220.

18 Mostowy S, Cousins D, Behr MA: Genomic interrogation of the dassie bacillus reveals it as a unique RD1 mutant within the *Mycobacterium tuberculosis* complex. *Journal of Bacteriology* 2004:186(1):104-109.

19 Murhead R, Burns K: Tuberculosis in wild badgers in Gloucestershire: epidemiology. *Veterinary Record 1974*:95(24):552-555.

20 Ofori-Anyinam B, Kanuteh F, Agbla SC, Adetifa I, Okoi C, Dolganov G, et al.: Impact of the *Mycobacterium africanum* West Africa 2 Lineage on TB Diagnostics in West

Africa: Decreased Sensitivity of Rapid Identification Tests in The Gambia. *PLoS Negl Trop Di*s 2016:10(7):e0004801.

21 Palomino J, Leao S, Ritacco V: Tuberculosis 2007 - From basic science to patient care. Amedeo Challenge:2007.

22 Parsons S, Drewe JA, Gey van Pittius NC, Warren RM, van Helden PD: Novel cause of tuberculosis in meerkats, South Africa. *Emerging Infectious Diseases* 2013:19(12):2004-2007.

23 Pym AS, Brodin P, Brosch R, Huerre M, Cole ST: Loss of RD1 contributed to the attenuation of the live tuberculosis vaccines *Mycobacterium bovis* BCG and *Mycobacterium microti*. *Molecular Microbiology* 2002:46(3):709-717.

24 Smith N: The 'Dassie' bacillus. Tubercle 1960:41(3):203-212.

25 Tiwari B, Soory A, Raghunand TR: An immunomodulatory role for the *Mycobacterium tuberculosis* region of difference 1 locus proteins PE35 (Rv3872) and PPE68 (Rv3873). *FEBS Journal* 2014:281(6):1556-1570.